Mechanical Reinforcement of Polymer Nanocomposites from Percolation of a Nanoparticle Network

Quan Chen,[†,‡] Shushan Gong,[†,‡] Joseph Moll,[§] Dan Zhao,[§] Sanat K. Kumar,[§] and Ralph H Colby*[,†]

[†]Department of Materials Science and Engineering, Pennsylvania State University, University Park, Pennsylvania 16802, United States
[§]Department of Chemical Engineering, Columbia University, 500 West 120th Street, New York, New York 10027, United States

S *Supporting Information*

ABSTRACT: Nanometer-sized particles that are well dispersed in a polymer melt, presumably due to strongly favorable particle–polymer interactions, can form fractal structures via polymer bridging, leading ultimately to a nanoparticle (NP) network analogous to a colloidal gel. The linear viscoelastic response of polymer nanocomposites can be quantitatively predicted by a parameter-free model in which the stress is a simple sum of contributions from the polymer matrix and the fractal NP structure linked by bridging polymer chains. The NP contribution is modeled using critical percolation, while the polymer part is enhanced by the presence of particles, owing to hydrodynamic interactions. The phase diagram at the right shows that small NPs are needed to achieve the stronger reinforcement from glassy bridges at reasonable particle loadings.
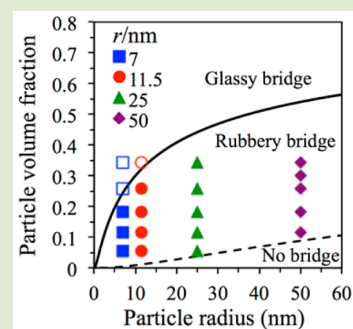
It is well-known that the addition of nanoparticles (NPs) can mechanically reinforce a polymer matrix.[1,2] The mechanism of reinforcement, however, remains in debate. At one extreme, Long and co-workers[3,4] used the fact that chain immobilization occurs around NPs; they suggested that mechanical reinforcement results when the NPs with the "bound" glassy layer percolate. A second scenario proposed by Goritz,[5] and elaborated by Sternstein,[6−8] is that the NPs form a flexible network, with the polymer chains forming the "bridges" between the NPs. A simple way to resolve the mechanism of reinforcement is to study NPs in a polymer melt far above T_g, in the limit where the chains and the NPs have a strong favorable interaction with each other. In this case, the improvement in mechanical properties on the addition of NPs can be described by critical percolation, as the polymer–particle bonds are effectively permanent (having lifetime much greater than 1000 s). With increasing NP concentration, there is a transition from a sol-like suspension, where NPs with their adsorbed bound polymers form separated branched structures, to a gel-like ensemble, where most NPs form a network percolating across the whole system.[1,9−11]

To understand this connectivity transition and its relationship to mechanical reinforcement, two basic questions should be addressed: (1) How do the NPs percolate? and (2) How is the percolation related to the mechanical properties? The first, "static", question can be asked in more specific ways as (a) What is the probability for a cluster to include n NPs? and (b) What is the size of the percolated structure? Although electron and atomic force microscopies have been frequently used to visualize such percolated NP structures,[1,2,12−14] it is difficult to define precisely the three-dimensional percolated structure.[1,2,12−14] Scattering is also frequently used to study the structure, in particular, the fractal dimension in reciprocal space. While

lower fractal dimension is reported for fumed silicas,[15] a fractal dimension of $d_f = 2.4 \pm 0.3$ is reported for aggregated silica-NPs,[16] consistent with the fractal dimension of 2.53 for critical percolation. Compared with experiments, simulation can more easily define the percolated structure,[11,12] but this result is found to strongly rely on the assumed interparticle potential. According to computer simulation combining mean-field theory with Monte Carlo simulations,[11] critical percolation theory is the relevant theory here in the strong interaction limit. The second question is on dynamics, which are also controlled by the interaction potential between NPs, but in the strong-interaction limit that we focus on here, where the interaction far exceeds the thermal energy k_BT, the bridges between particles become effectively permanent on the time scale of our measurements.

Here, an analytical theory is developed to predict the linear viscoelasticity corresponding to the sol−gel transition of NPs based on critical percolation.[17] We assume that the complex modulus of the nanocomposite is the sum of two contributions: one from the surrounding polymer matrix and the other from the particle network bridged by polymer chains, that is, $G^*(\omega) = G^*_{polymer}(\omega) + G^*_{PN}(\omega)$.

The simplest assumption, which follows from recent computer simulations, is that the modulus of the polymer with the NPs has the same mode distribution of relaxation times as the bulk polymer: $G^*_{polymer} = \kappa G^*_{bulk}$, where κ (>1) is a factor characterizing the increase in the polymer's modulus due to the presence of the NPs. In general, κ can be expressed as a function of filler volume fraction ϕ, $\kappa = G^*_{polymer}/G^*_{bulk} = 1 + c_1\phi$

$+ c_2\phi^2 + ...$ Einstein, Batchelor, and Brady analyzed the effect of hydrodynamic interaction with immobile particles to conclude $c_1 = 2.5$ and $c_2 = 5.2-7$.[10,18-20] Nevertheless, higher order terms having unknown coefficients also contribute to κ, especially at high ϕ.[9,10,21-23] To address this problem, phenomenological equations such as the Guth−Gold equation or Krieger−Dougherty equation are frequently used as substitutes.[24,25]

Here, an effective volume fraction ϕ_{eff} is calculated by accounting for the fact there exists an interfacial region where segmental mobility of polymer chains is greatly reduced. The existence of this interfacial bound layer has been suggested by various experimental techniques.[14,26-32] The bound layer thickness was reported to vary between $\delta = 1-5$ nm depending on the size of spherical NPs, chemistry of polymer, and strength of NPs/polymer interaction. In good agreement, our recent studies using TGA and dielectric spectroscopy suggest $\delta = 1-4$ nm for the silica/poly(2-vinylpyridine) nanocomposites, the model systems studied in this letter.[14,33] Due to the immobile bound layer, the effective filler volume fraction would be $\phi_{eff} = \phi(r + \delta)^3/r^3$ for NPs with bound polymer.

In summary, the modulus of the polymer matrix is expressed by the Guth-Gold equation as[24]

$$G^*_{polymer} = \kappa G^*_{bulk} \tag{1a}$$

$$\kappa = 1 + 2.5\phi_{eff} + 14.1\phi_{eff}^2, \quad \text{with } \phi_{eff} = \phi(r + \delta)^3/r^3 \tag{1b}$$

The particle network part of the modulus is expressed using the static and dynamic scaling of critical percolation:[34,35] (1) The number density of clusters of n NPs is $P(n) \sim n^{-\tau}$ for $1 \leq n \leq n_{char}$ with $\tau = 2.2$ for critical percolation; $n_{char} \sim |\phi-\phi_c|^{-1/\sigma}$ with ϕ_c being the volume fraction of NPs at the gel point, and $\sigma = 0.45$ for critical percolation. (2) The cluster size R of associated NPs as a function of n is $R(n) \sim n^{1/d_f}$, with d_f the fractal dimension (larger d_f means a denser structure; $d_f = 2.5$ for critical percolation). (3) The cluster's relaxation rate $\varepsilon(n) \sim D(n)/[R(n)]^2 \sim n^{-(2+d_f)/d_f}$, where $D(n) \sim n^{-1}$ is the diffusion coefficient of a cluster containing n NPs.

The modulus at the relaxation time of a cluster of n NPs is proportional to the fraction of clusters having more than n NPs: $G_{PN}(n) \sim n^{-1} \int_n^{n_{char}} nP(n)dn \sim n^{-\tau+1}$, assuming that the number of relaxation modes of each cluster is proportional to n. A combination of $G_{PN}(n) \sim n^{-\tau+1}$ and relaxation frequency $\varepsilon(n) \sim n^{-(2+d_f)/d_f}$ gives $G_{PN}(t) \sim t^{-d_f(\tau - 1)/(2 + d_f)}$ ($\sim t^{-2/3}$ for critical percolation), meaning $G^*_{PN} \sim (i\omega)^u$ with $u = d_f(\tau - 1)/(2 + d_f) = 2/3$ for critical percolation in the frequency domain. More specifically, the complex modulus of the particle network G^*_{PN} can be written as eq 2a when the NPs have not yet formed a percolated network (i.e., below the gel point), and eq 2b when the network has been formed (above the gel point):[34]

$$G^*_{PN}(\omega) = \frac{i\omega G_{PN}}{1 - n_{char}^{2-\tau}}\left[\int_{\varepsilon_{char}}^{\varepsilon_0} \frac{(\varepsilon/\varepsilon_0)^{d_f(\tau-1)/(2+d_f)}}{i\omega + \varepsilon}\frac{d\varepsilon}{\varepsilon}\right.$$
$$\left. - n_{char}^{2-\tau}\int_{\varepsilon_{char}}^{\varepsilon_0} \frac{(\varepsilon/\varepsilon_0)^{d_f/(2+d_f)}}{i\omega + \varepsilon}\frac{d\varepsilon}{\varepsilon}\right] \text{ for } \phi < \phi_c \tag{2a}$$

$$G^*_{PN}(\omega) = G_{PN}\left[i\omega \int_{\varepsilon_{char}}^{\varepsilon_0} \frac{(\varepsilon/\varepsilon_0)^{d_f(\tau-1)/(2+d_f)}}{i\omega + \varepsilon}\frac{d\varepsilon}{\varepsilon} + n_{char}^{1-\tau}\right] \text{ for } \phi \geq \phi_c \tag{2b}$$

with (I) $d_f = 2.5$, $\tau = 2.2$ for critical percolation. (II) $n_{char} \cong |\phi - \phi_c|^{-1/\sigma}$, with $\sigma = 0.45$ for critical percolation and ϕ_c specifying the volume fraction corresponding to the gel point. (III) $\varepsilon_0 = 1/\tau_d$ and $\varepsilon_{char} \cong \varepsilon_0 n_{char}^{-(2 + d_f)/d_f}$, with τ_d being the terminal relaxation time of the surrounding polymer matrix. The former equation is reasonable when particle size is larger than the entanglement mesh size of the polymer matrix.

In eq 2, the amplitude G_{PN} is the only parameter to be specified. To this end, focus is placed on the modulus per particle, that is, G_{PN} normalized by $\nu_{particle}kT$, with $\nu_{particle}$ being the number density of particles.[36-38] Previous studies revealed a power law dependence $G_{PN} \sim \phi^{\,m}$, with $m \approx 3-5$ for strong particle−particle interactions.[9] In this study, the particles bridged by polymer chains are assumed to store the stress, with $G_{PN} = \nu_{particle}k_BTn_b$[36-38] and n_b the number of bridges per particle. de Gennes predicted that the density (number per area) of bridging chains $\sim h^{-2}$, where $h = rf(\phi)$ is the distance between two plates of size r. Then, the number of bridges per particle is $n_b = S/h^2 = 4\pi r^2/\{rf(\phi)\}^2 = 4\pi/f(\phi)^2$, with $S = 4\pi r^2$ the surface area of each particle.[39]

Considering a particle should occupy a volume of $V \sim r^3/\phi$, the average distance between particle surfaces would be $h_{av} = V^{1/3} - 2r \approx 2r(\phi^{-1/3} -1)$, that is, $f(\phi) = 2\phi^{-1/3} - 2$. Nevertheless, particles are not uniformly distributed and bridge density should be controlled by the mean nearest-neighbor distance. Torquato, Lu, and Rubinstein analyzed the nearest neighbor probability density function to obtain an expression allowing numerical calculation of the mean nearest-neighbor distance as[40]

$$h_{near} = 2r\int_1^\infty \exp\{-\phi[8(1 + \phi)(x^3 - 1) - 6\phi(3 + \phi)$$
$$(x^2 - 1) + 12\phi^2(x - 1)]/(1 - \phi)^3\}dx \tag{3}$$

where h_{near} can be analytically approximated[40] for $\phi > 0.2$ as $h_{near} \approx r(1 - \phi)^3/[6\phi(2 - \phi)]$, see equation 6.12 of ref 40.

(IV) the amplitude $G_{PN} = \nu_{particle}k_BTn_b$, with $n_b \cong 4\pi r^2/h_{near}^2$. This expression is valid only if h_{near} is in the range between segment size b and chain size R of the matrix. Since the mean size of bridging chains is $\sim h_{near}$, the volume per bridge is $(h_{near}^2/b^2) \times b^3$, and the ratio of volume of bridges per particle and particle volume $V_{particle} = 4\pi r^3/3$ is $\sim n_b \times (h_{near}^2/b^2) \times b^3/V_{particle} = 3b/r$, meaning that the volume fraction of bridging chains is $3\phi b/r$, which is usually smaller than ϕ since $b < r/3$.

Figure 1 schematically illustrates $G'_{polymer}$ and G'_{PN} as functions of angular frequency ω based on critical percolation. With NPs present, $G'_{polymer}$ has the same relaxation frequency,
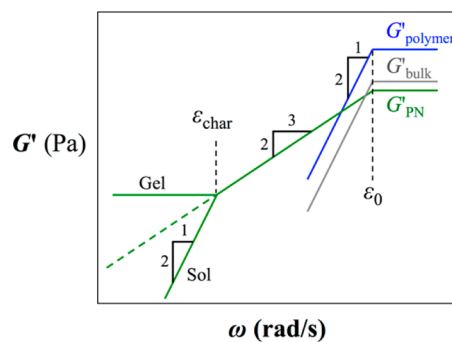

Figure 1. Schematic illustration of polymer and particle network components of storage modulus as functions of angular frequency ω.

ε_0, but larger amplitude compared with that of the bulk polymer, from hydrodynamic coupling with the less mobile NPs. The relaxation of the NP clusters G'_{PN} is activated by that of $G'_{polymer}$. G'_{PN} then has a power law viscoelasticity with slope 2/3 that continues until the cutoff frequency ε_{char} of the largest cluster, followed by either a terminal relaxation below the gel point or a network modulus above the gel point.

To test the validity of this model of mechanical relaxation for nanocomposites, silica NPs (Nissan Chemicals) with various radii r (=7, 11.5, 25, and 50 nm) were well-dispersed in a poly(2-vinylpyridine) matrix (P2VP from Polymer Source, M_n = 97000; M_w/M_n = 1.08; T_g = 371 K), with the weight fractions w of NPs varied from 0 to 50 wt %, corresponding to volume fractions ϕ up to 34%. The P2VP is chosen due to its strong hydrogen bonding interaction to the silica surface, which facilitates the uniform dispersion of the NPs in the polymer.[1,14] We believe that a bound layer of polymer with a long lifetime forms at the particle surface, allowing the polymer bridges to be permanent on the time scales of our measurements.

The samples were prepared by solution casting from either 2-butanone (for r = 7 and 25 nm silica) or isopropanol (for r = 11.5 and 50 nm silica) with pyridine (Sigma-Aldrich) as dispersant.[14] Ultrasonication was applied in solution to improve dispersion of nanoparticles, confirmed by TEM in our previous study. The cast samples were first annealed under vacuum for 7 days at 80 °C and then 10 days at 150 °C prior to being molded into ~1 mm thick and 7.9 mm diameter discs. Linear viscoelastic (LVE) measurements were conducted, under N_2, for those discs between 7.9 mm diameter parallel plates on an Advanced Rheometric Expansion System ARES-LS1 rheometer (Rheometric Scientific) at 180 °C. The linear strain amplitudes were verified by strain amplitude sweeps.

Figure 2 shows the linear viscoelastic storage and loss moduli, G' and G'', as functions of angular frequency ω for silica NPs (r = 7, 11.5, 25, and 50 nm) dispersed in the P2VP matrix at T = 180 °C. At the highest frequencies studied, the modulus of nanocomposites increases with the volume fraction of NPs, the increase becomes weaker with increasing particle size. At ω lower than the terminal relaxation of the polymer, an additional stress component manifests: For low NP content (ϕ = 6%), a transition from power law to terminal relaxation can be observed, corresponding to relaxation of nanoparticle clusters below their gel point. Finally, at high content of nanoparticles, a low ω plateau can be observed, reflecting the formation of a percolated NP-network (gel). The thin solid curves in Figure 2 are predictions from the proposed model. The overall agreement between experimental results and model predictions is remarkable, supporting the molecular view that the NP gelation obeys critical percolation with bridging chains[5−8] bearing the stress as long as the mean nearest-neighbor distance between particles is larger than the Kuhn length. Nevertheless, deviations can be clearly seen at high loading of small NPs, which we will understand below.

For the polymer part of the modulus, the bound layer thickness δ gives the effective volume fraction ϕ_{eff}. Since our recent studies suggest δ = 1−4 nm for the same silica/P2VP nanocomposites, a reasonable choice δ = 2 nm is made here for all the nanocomposites.[14,33]

For the particle network component of the modulus, the gel point must first be determined. In LVE, the gel point is identified from a low frequency power law as $G' \sim G'' \sim \omega^u$, with u = 2/3 for critical percolation.[35,41−44] This feature allows determination of ϕ_c, where G' and $G''/\tan(\pi/3)$ cross at low
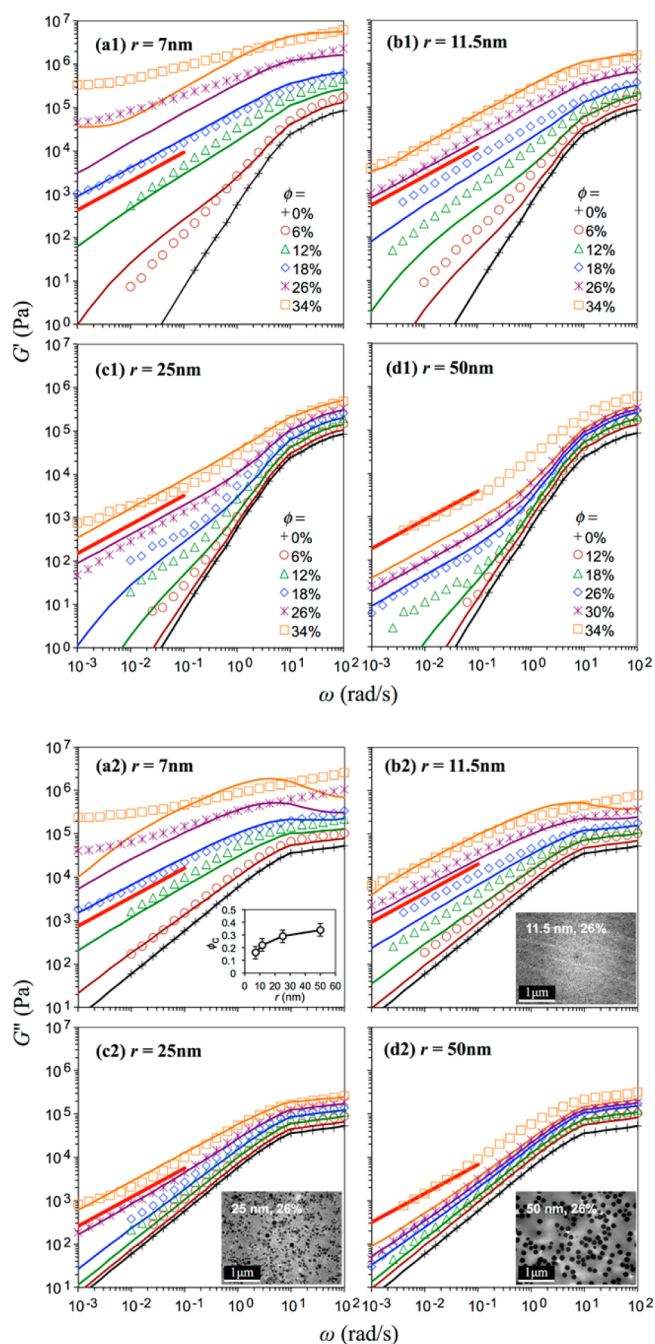

Figure 2. Storage modulus G' (top panels) and loss modulus G'' (bottom panels) at 180 °C, of silica/P2VP nanocomposites with particle sizes r = 7, 11.5, 25, and 50 nm and volume fraction ϕ as indicated. Thin solid curves are predictions. Thick solid lines indicate the lines $G' \sim G'' \sim \omega^u$, with G''/G' = $\tan(u\pi/2)$ and u = 2/3 for critical percolation expected at the gel point ϕ_c. Inset of panel (a2) shows the dependence of ϕ_c on particle size r of the volume fraction of NPs at the gel point. ϕ_c is determined from raw G' and G'' data at low ω, as explained in Figure S1 of Supporting Information. Insets of panels (b2), (c2), and (d2) are TEM images of the nanocomposites with ϕ = 26%.

frequency, as explained in Figure S1 of Supporting Information, which yields ϕ_c = 16, 22, 29, and 34 (±5)% for r = 7, 11.5, 25, and 50 nm, respectively. ϕ_c is plotted against r in the inset of Figure 2(a2). The powers $G' \sim G'' \sim \omega^{2/3}$ at the gel point ϕ_c are shown in thick red solid lines in Figure 2. Meanwhile, the

characteristic time for particle motion (III) $\varepsilon_0 = 1/\tau_d$ is reasonable when NPs are considerably larger than the entanglement mesh size of the polymer matrix. Here, the diameter of particles $2r \geq 14$ nm is larger than entanglement length $a = 13$ nm for P2VP (calculated from $a^2 = M_e\langle R^2\rangle/M$, with $\langle R^2\rangle/M = 6.6 \times 10^{-3}$ nm^2 for P2VP in a θ solvent[45] and $M_e = 27000$ for P2VP[46]).

In addition, (IV) $G_{PN} \cong \nu_{particle}k_B T n_b$, with $n_b = 4\pi r^2/h_{near}^2$ is based on an assumption of flexible bridges: this assumption is valid only if h_{near} is in between the segment and chain sizes of the matrix polymer, i.e., in between Kuhn length $b \approx 1$ nm and the end-to-end distance $R = 25$ nm (see Figure S2 of Supporting Information).[3,4] In other words, the particles should neither be too crowded, so that the bridges remain flexible, nor too sparse, so that particle−particle bridges can form. We define two critical concentrations ϕ^* and ϕ^{**}, at which $h_{near} = b$ and R, respectively. Using the analytical approximation $b = h_{near} \approx r(1 - \phi^*)^3/[6\phi^*(2 - \phi^*)]$ (the asymptotic expression of eq 3 can be used since $\phi^* > 0.2$ is expected), there is an analytical solution for ϕ^*:

$$\phi^* = 1 + 2b/r - b^2/\{r^2 g(b/r)\} - g(b/r),$$
$$\text{with } g(x) = \{-8x^3 + (9x^2 - 48x^4)^{1/2} + 3x\}^{1/3} \quad (4)$$

In Figure 3, ϕ is plotted against r for all nanocomposites in this study to create a phase diagram. ϕ^* and ϕ^{**} from
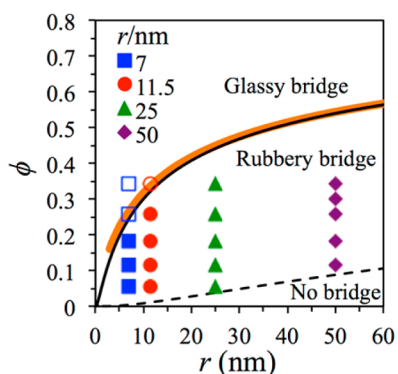

Figure 3. Concentration ϕ plotted against particle size r (symbols). Thin solid and thin dashed black curves represent critical concentration ϕ^* and ϕ^{**} obtained from numerical calculation (eq 3), at which the mean nearest-neighbor spacing equals the Kuhn length $b = 1$ nm and chain size $R = 25$ nm, respectively. Thick solid orange curve is ϕ^* from analytical calculation (eq 4).

numerical calculation (eq 3) are shown as the thin solid black and dashed curves, respectively, while ϕ^* from eq 4 is shown as a thick solid orange curve for comparison. Both ϕ^* and ϕ^{**} increase with r, where ϕ^* separates regimes of rubbery flexible bridges and glassy bridges, and ϕ^{**} separates flexible bridge and no bridge regimes. It is obvious that all the nanocomposites in this study have sufficient particle concentration for bridges to form. Nevertheless, for small particles at high loading, the bridges are predicted to become nonflexible and glassy, see the unfilled symbols for $\phi \geq \phi^*$ ($h_{near} \leq b$), which is likely responsible for the failure of our prediction for the two highest content samples with $r = 7$ nm, and the highest content sample with $r = 11.5$ nm in Figure 2, considering that rubbery bridges is one vital assumption of our flexible percolation model. Not surprisingly, the data for $\phi = 26\%$ and 34% of the $r = 7$ nm NPs in Figures 2(a1) and 2(a2) are significantly above the flexible

bridge percolation model predictions, as these have some mixture of flexible and more rigid glassy bridges between NPs.

In summary, a parameter free analytical model is proposed to predict the LVE of hydrophilic NPs well-dispersed in a polar polymer matrix with strong interactions between the particles and the polymer, using critical percolation of NPs. This model is applicable for particles that are neither too crowded nor too sparse, so that the flexible bridges form between particles. The limit where particles form glassy bridges when they are too close is evident in our LVE data for small NPs at high loading, exactly as anticipated by our phase diagram (Figure 3) and perhaps described by other models,[3,4] but that is left for future work.

■ ASSOCIATED CONTENT

Ⓢ Supporting Information
Figure S1: determination of the gel point; Figure S2: comparison of the mean nearest-neighbor distance h_{near} between particles and segment and chain sizes of the polymer matrix. This material is available free of charge via the Internet at http://pubs.acs.org.

■ AUTHOR INFORMATION

Corresponding Author
*E-mail: rhc@plmsc.psu.edu.

Author Contributions
‡These authors contributed equally to this work and are cofirst authors (Q.C. and S.G.).

Notes
The authors declare no competing financial interest.

■ ACKNOWLEDGMENTS

■ REFERENCES

(1) Kumar, S. K.; Krishnamoorti, R. *Annu. Rev. Chem. Biomol.* **2010**, *1*, 37.
(2) Moll, J. F.; Akcora, P.; Rungta, A.; Gong, S. S.; Colby, R. H.; Benicewicz, B. C.; Kumar, S. K. *Macromolecules* **2011**, *44*, 7473.
(3) Long, D.; Sotta, P. *Rheol. Acta* **2007**, *46*, 1029.
(4) Long, D.; Lequeux, F. *Eur. Phys. J. E* **2001**, *4*, 371.
(5) Maier, P. G.; Goritz, D. *Kautsch. Gummi Kunstst.* **1996**, *49*, 18.
(6) Zhu, A. J.; Sternstein, S. S. *Compos. Sci. Technol.* **2003**, *63*, 1113.
(7) Sternstein, S. S.; Zhu, A. J. *Macromolecules* **2002**, *35*, 7262.
(8) Sternstein, S. S.; Ramorino, G.; Jiang, B.; Zhu, A. J. *Rubber Chem. Technol.* **2005**, *78*, 258.
(9) Larson, R. G. *The Structure and Rheology of Complex Fluids*; Oxford University Press: New York, 1999.
(10) Mewis, J.; Wagner, N. J. *Colloidal Suspension Rheology*; Cambridge University Press: Cambridge ; New York, 2012.
(11) Surve, M.; Pryamitsyn, V.; Ganesan, V. *Phys. Rev. Lett.* **2006**, *96*.
(12) Akcora, P.; Liu, H.; Kumar, S. K.; Moll, J.; Li, Y.; Benicewicz, B. C.; Schadler, L. S.; Acehan, D.; Panagiotopoulos, A. Z.; Pryamitsyn, V.; Ganesan, V.; Ilavsky, J.; Thiyagarajan, P.; Colby, R. H.; Douglas, J. F. *Nat. Mater.* **2009**, *8*, 354.
(13) Akcora, P.; Kumar, S. K.; Moll, J.; Lewis, S.; Schadler, L. S.; Li, Y.; Benicewicz, B. C.; Sandy, A.; Narayanan, S.; Illavsky, J.; Thiyagarajan, P.; Colby, R. H.; Douglas, J. F. *Macromolecules* **2010**, *43*, 1003.
(14) Jouault, N.; Moll, J. F.; Meng, D.; Windsor, K.; Ramcharan, S.; Kearney, C.; Kumar, S. K. *ACS Macro Lett.* **2013**, *2*, 371.
(15) Schaefer, D. W.; Justice, R. S. *Macromolecules* **2007**, *40*, 8501.
(16) Baeza, G. P.; Genix, A.-C.; Degrandcourt, C.; Petitjean, L.; Gummel, J.; Couty, M.; Oberdisse, J. *Macromolecules* **2013**, *46*, 317.

(17) Stauffer, D.; Aharony, A. *Introduction to Percolation Theory*, 2nd ed.; Taylor & Francis: London ; Washington, DC, 1992.

(18) Batchelor, G. K.; Green, J. T. *J. Fluid Mech.* **1972**, *56*, 375.

(19) Wagner, N. J.; Woutersen, A. T. J. M. *J. Fluid Mech.* **1994**, *278*, 267.

(20) Bergenholtz, J.; Brady, J. F.; Vicic, M. *J. Fluid Mech.* **2002**, *456*, 239.

(21) Chong, J. S.; Christiansen, E. B.; Baer, A. D. *J. Appl. Polym. Sci.* **1971**, *15*, 2007.

(22) Song, Y. H.; Zheng, Q. *Polymer* **2011**, *52*, 593.

(23) Song, Y. H.; Zheng, Q. *Polymer* **2011**, *52*, 6173.

(24) Guth, E.; Gold, O. *Phys. Rev.* **1938**, *53*, 322.

(25) Krieger, I. M.; Dougherty, T. J. *Trans. Soc. Rheol.* **1959**, *3*, 137.

(26) Bershtein, V. A.; Egorova, L. M.; Yakushev, P. N.; Pissis, P.; Sysel, P.; Brozova, L. *J. Polym. Sci., Polym. Phys.* **2002**, *40*, 1056.

(27) Chen, K. H.; Yang, S. M. *J. Appl. Polym. Sci.* **2002**, *86*, 414.

(28) Rittigstein, P.; Priestley, R. D.; Broadbelt, L. J.; Torkelson, J. M. *Nat. Mater.* **2007**, *6*, 278.

(29) Liu, X. H.; Wu, Q. J. *Polymer* **2001**, *42*, 10013.

(30) Fragiadakis, D.; Pissis, P.; Bokobza, L. *Polymer* **2005**, *46*, 6001.

(31) Ash, B. J.; Schadler, L. S.; Siegel, R. W. *Mater. Lett.* **2002**, *55*, 83.

(32) Walden, P. *Z. Phys. Chem.* **1906**, *55*, 207.

(33) Gong, S.; Chen, Q.; Moll, J. F.; Kumar, S. K.; Colby, R. H. *ACS Macro Lett.* **2014**, *3*, 773.

(34) Rubinstein, M.; Colby, R. H.; Gillmor, J. R. *Dynamics of Near-Critical Polymer Gels*; Springer-Verlag: Berlin; New York, 1989; Vol. 51.

(35) Rubinstein, M.; Colby, R. H. *Polymer Physics*; Oxford University Press: New York, 2003.

(36) Aranguren, M. I.; Mora, E.; Degroot, J. V.; Macosko, C. W. *J. Rheol.* **1992**, *36*, 1165.

(37) Zhu, Z. Y.; Thompson, T.; Wang, S. Q.; von Meerwall, E. D.; Halasa, A. *Macromolecules* **2005**, *38*, 8816.

(38) Otsubo, Y.; Nakane, Y. *Langmuir* **1991**, *7*, 1118.

(39) de Gennes, P. G. *Adv. Colloid Interface* **1987**, *27*, 189.

(40) Torquato, S.; Lu, B.; Rubinstein, J. *Phys. Rev. A* **1990**, *41*, 2059.

(41) Derosa, M. E.; Winter, H. H. *Rheol. Acta* **1994**, *33*, 220.

(42) Chen, Q.; Colby, R. H. *Korea−Australia Rheol. J.* **2014**, *26*, 257.

(43) Chen, Q.; Huang, C.; Weiss, R. A.; Colby, R. H. *Macromolecules* **2015**, *48*, 1221.

(44) Lusignan, C. P.; Mourey, T. H.; Wilson, J. C.; Colby, R. H. *Phys. Rev. E* **1995**, *52*, 6271.

(45) Brandrup, J.; Immergut, E. H.; Grulke, E. A. *Polymer Handbook*, 4th ed.; Wiley: New York, 1999.

(46) Tan, N. C. B.; Peiffer, D. G.; Briber, R. M. *Macromolecules* **1996**, *29*, 4969.